Mechanics of Time-Dependent Materials (2023) 28:663–680
https://doi.org/10.1007/s11043-023-09603-1

RESEARCH

Free vibration of foam plates on viscoelastic foundations considering thickness stretching

H.A. Zamani[1] · **M. Salehi**[1]

Received: 21 March 2023 / Accepted: 2 May 2023 / Published online: 17 May 2023

Abstract
In this work, we study the thickness-stretching effects for vibrational behaviors of open-cell foam plates resting on the visco-Pasternak foundation. The kinematic relations consist of shear and normal deformation theory with hyperbolic functions and normal strains in the thickness directions. These relations of foam plates are extended here for the first time. We derive the porosity distribution, viscoelastic constitutive relations, and the governing equations with frequency-dependent coefficients using power law, Boltzmann–Volterra superposition principles, and the Hamilton principle, respectively. We derive natural frequencies and modal loss factors of simply supported thick plates based on a semianalytical solution and numerical iterative algorithm. To verify, we carry some numerical examples for elastic functionally graded plates and viscoelastic laminated composite plates. We study the influences of geometry, material, and foundation parameters through numerical examples. It is revealed that loss factors of thin plates show increment as both thickness ratio and viscoelastic coefficients increase because external damping dominates over structural damping.

Keywords Open-cell foams · Functionally graded foam · Shear and normal deformation theory · Semianalytical solution

1 Introduction

Functionally graded (FG) foams have attracted great attention due to the remarkable simultaneous properties of FG and viscoelastic materials (Altenbach and Eremeyev 2009, 2008a,b,c). Functionally graded materials have degraded properties that avoid severe variations of properties and thermo-mechanical stresses, and viscoelastic materials have high damping capability and phase delay (Brinson and Brinson 2008). Viscoelastic materials also can provide safe and quick ophthalmic surgery (Buratto et al. 2000). These foams are generally known as FG viscoelastic (FGV) foams and are categorized based on their inner connections, the open-cell with interconnected networks of cells, and close-cell without interconnections of cells (Ashby et al. 2000; Taraz Jamshidi et al. 2015; Hedayati and Sadighi 2016; Sadeghnejad et al. 2017; Sarrafan and Li 2022).

✉ H.A. Zamani
zamani.h.a@aut.ac.ir

[1] Mechanical Engineering Department, Amirkabir University of Technology (Tehran Polytechnic), 424 Hafez Ave., Tehran, 15875-4413, Iran

The mentioned properties of FGV foams provide an opportunity to use them in beam, plate, and shell structures, as a whole or as a constituent of composites (Jahwari and Naguib 2016; Zamani 2021a; Montgomery et al. 2021). From this point of view, FGV plates under dynamic loads are newly at the center of the attentions of researchers. Hosseini-Hashemi et al. (2015) used first-order shear deformation theory (FSDT) to derive natural frequency and damping ratios of cylindrical panels under Levy-type boundary conditions. Shariyat and Jahangiri (2020) studied the impact behavior of partially supported plates under bending-induced fluid flow based on the Galerkin finite element method (FEM) and the Hertz law. Zamani (2021b) applied the Galerkin, least squares, Ritz, and point collocation weighted residual methods to derive complex frequencies of foam plates. Alavi et al. (2022) studied transient and dynamic responses of porous standard solid plates using FSDT and the perturbation method. Dogan (2022) investigated quasi-static and dynamic responses of plates based on modified Durbin's algorithm and Navier approach. Zamani (2022) considered thickness-stretching effect for free vibrations of thick foam plates using the Galerkin method with various shear and normal deformation theories (SNDT). Singh et al. (2023) applied power series EKM for standard solid piezoelectric plates with Levy-type boundary conditions.

In many practical circumstances, interactions of the foundation are inevitable (Kerr 1964). Therefore FGV plates may face various loads such as elastic and viscoelastic foundations. In this outline, Alimirzaei et al. (2019) investigated wave propagation of FGV plates on the visco-Pasternak foundation using a quasi-3D shear deformation theory. Sofiyev et al. (2019) analyzed the dynamic buckling of plates resting on an elastic foundation based on the CPT and the Galerkin method. Also, Sofiyev (2023) extended the dynamic buckling investigation for plates on viscoelastic foundation under different initial conditions. Besides FGV plates, vibration behavior of FGV foams on foundations is taken into consideration in recent years. Zamani et al. (2018) studied the free vibration of thin foam plates on an orthotropic foundation based on the classical plate theory (CPT), the Galerkin method, and various boundary conditions. Recently, Zamani et al. (2022) studied large-amplitude vibrations and mechanical buckling of foam beams on a nonlinear elastic foundation. They concluded that the viscoelasticity of foams enhances the differences of linear and nonlinear frequencies and buckling loads. Obviously, vibration analysis of FGV foam plates on the viscoelastic foundation is limited to the thin plates and CPT, whereas in many practical circumstances, analysis of thick plates using SNDT considering thickness-stretching effects are necessary. Furthermore, the main aim of this study is the implementation of viscoelastic foundation for vibrations of thick foam plates considering thickness stretching.

In accordance with the literature review, it is revealed that dynamic analysis of FGV plates is restricted to the CPT (Shariyat and Jahangiri 2020; Dogan 2022), FSDT (Hosseini-Hashemi et al. 2015; Alavi et al. 2022), refined FSDT (Zamani 2021b), quasi-3D theories (Singh et al. 2023), and SNDT (Zamani 2022). Moreover, dynamic analysis of FGV plates on foundations (Sofiyev et al. 2019; Sofiyev 2023) and FGV foams on foundations (Zamani et al. 2018, 2022) is limited to the CPT and wave propagation with quasi-3D (Alimirzaei et al. 2019) approach. Overall, there is no study for the application of SNDT for vibrations of thick shear-and-normal deformable FGV foam plates resting on the viscoelastic foundations.

In this paper, SNDT is applied to study the complex frequency behavior of foam plates. Shear and normal deformation theory includes in-plane and out-of-plane displacements, whereas normal strain through the thickness direction is also considered. Simple power law, separable kernels framework, and Boltzmann–Volterra superposition integral are adapted for constitutive relations. The Hamilton principle is used to derive the governing equations of motions with frequency-dependent coefficients. The Galerkin method in conjunction with

QZ iterative numerical algorithm is implemented to derive natural frequencies and modal loss factors. Some numerical examples are carried out to assess the accuracy of the present method. Then the impacts of material model, geometrical parameters, and foundation coefficients are investigated through parametric studies.

2 Basic formulation

Consider a rectangular plate as depicted by Fig. 1. Variables x, y, and z stand for orthogonal coordinate systems, and the origin is placed at the corner of the midsurface of the plate. The parameters a, b, and h denote the length, width, and total thickness, respectively. Moreover, K_w, K_p, and K_d represent the Winkler, Pasternak, and damping coefficients of foundation, respectively.

2.1 Constitutive equations

In the present work, we adapt the Boltzmann–Volterra superposition integral is adapted for linear viscoelastic behavior of the open-cell foam plate as follows (Brinson and Brinson 2008):

$$\begin{Bmatrix} \sigma_{xx} \\ \sigma_{yy} \\ \sigma_{zz} \\ \sigma_{yz} \\ \sigma_{xz} \\ \sigma_{xy} \end{Bmatrix} = \int_{-\infty}^{t} \begin{bmatrix} \lambda_1(t-t') & \lambda(t-t') & \lambda(t-t') & 0 & 0 & 0 \\ & \lambda_1(t-t') & \lambda(t-t') & 0 & 0 & 0 \\ & & \lambda_1(t-t') & 0 & 0 & 0 \\ & Sym. & & \mu(t-t') & 0 & 0 \\ & & & & \mu(t-t') & 0 \\ & & & & & \mu(t-t') \end{bmatrix} \times \begin{Bmatrix} \varepsilon_{x,t'}(t') \\ \varepsilon_{y,t'}(t') \\ \varepsilon_{z,t'}(t') \\ \varepsilon_{yz,t'}(t') \\ \varepsilon_{xz,t'}(t') \\ \varepsilon_{xy,t'}(t') \end{Bmatrix} dt', \tag{1}$$

where σ, ε, t, t', and "," stand for the stress, strain, time, Boltzmann integral variable, and differential operator, respectively. Moreover, λ, λ_1, and μ represent frequency-dependent viscoelastic Lame coefficients (Brinson and Brinson 2008; Altenbach and Eremeyev 2008b,c):

$$\begin{aligned} \lambda(z,\omega) &= K(z\omega) - \frac{2}{3}G(z,\omega) = \frac{\nu(z,\omega)E(z,\omega)}{(1-2\nu(z,\omega))\,(1+\nu(z,\omega))}, \\ \lambda_1(z,\omega) &= K(z,\omega) + \frac{4}{3}G(z,\omega) = \frac{(1-\nu(z,\omega))}{\nu(z,\omega)}\lambda(z,\omega), \end{aligned} \tag{2}$$

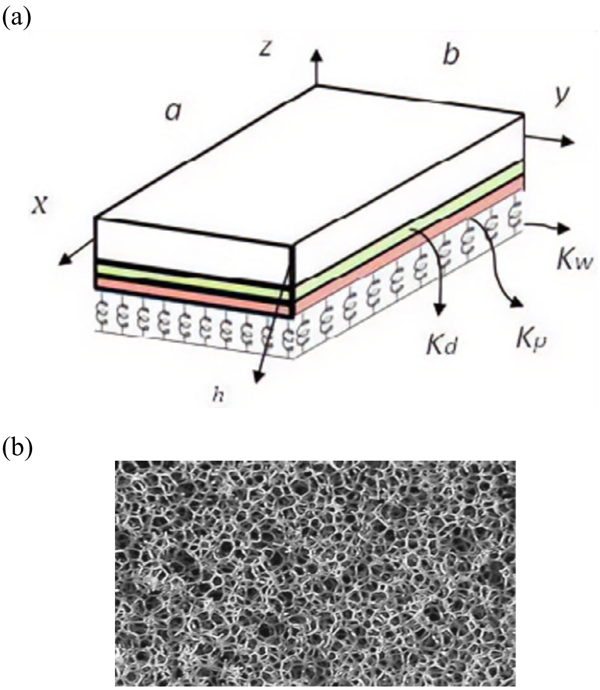

Fig. 1 The geometry and coordinates of a functionally graded viscoelastic plate (a) and schematic of a polymeric open-cell foam (b) (Altenbach and Eremeyev 2008c)

$$\mu(z,\omega)=G(z,\omega)=\frac{E(z,\omega)}{2(1+\nu(z,\omega))},$$

$$\lambda\left(\omega,z\right)+2\mu\left(\omega,z\right)=\lambda_1\left(\omega,z\right),$$

$$\hat{C}_{12}\left(\omega\right)+2\hat{C}_{66}\left(\omega\right)=\hat{C}_{11}\left(\omega\right),$$

$$\hat{C}_{11}\left(\omega\right)=\hat{C}_{22}\left(\omega\right)=\hat{C}_{33}\left(\omega\right),$$

$$\hat{C}_{13}\left(\omega\right)=\hat{C}_{23}\left(\omega\right)=\hat{C}_{12}\left(\omega\right),$$

$$\hat{C}_{44}\left(\omega\right)=\hat{C}_{55}\left(\omega\right),$$

where ω, K G, E, C, and ν stand for the frequency, bulk, shear, Young moduli, viscoelastic stiffness coefficients, and Poisson ratio, respectively. Generally, the mentioned properties are frequency-dependent or time-dependent, and in the present study, we consider the frequency-dependent one. Also, frequency-dependent properties and viscoelastic stiffness coefficients could be derived directly using the Alfrey correspondence principle (Alfrey 1944). Other effective properties could be written as (Srinivas and Rao 1971; Hatami et al. 2008)

$$\rho\left(z,\omega\right)=\rho_s V\left(z\right), \tag{3}$$

$$K\left(z,\omega\right)=K_0 V^2\left(z\right), \tag{4}$$

$$G\left(z,\omega\right)=G_0\frac{1+ic_1\omega}{1+i\beta c_1\omega}V^2\left(z\right), c_1=h\sqrt{\frac{\rho}{G_0}}, \tag{5}$$

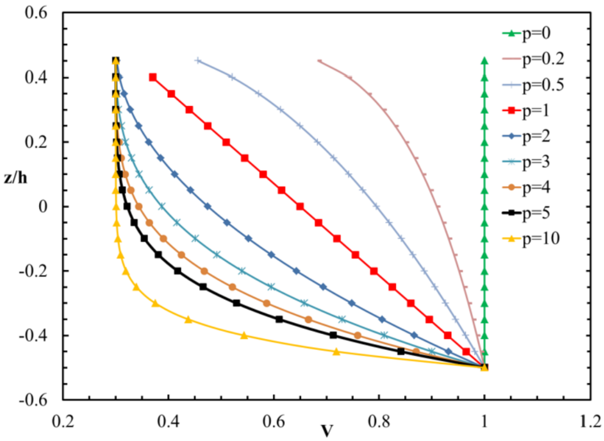

Fig. 2 The effects of power index on volume fraction (Zamani et al. 2018)

$$V(z) = \frac{\rho_p}{\rho_s} + (1 - \frac{\rho_p}{\rho_s})(\frac{1}{2} - \frac{z}{h})^p, \tag{6}$$

where ρ, ρ_s, ρ_p/ρ_s, p, β, K_0, and G_0 stand for the density, minimum density, minimal relative density, power index, parameter of constitutive relation, elastic dilatation, and distortion moduli, respectively. Also, $\beta = 0.5, 1$ and $p = 0, 1, 2$ represent standard solid and elastic models, and homogenous, linear, and quadratic distributions of porosity through the thickness direction, respectively. It is worth mentioning that homogenous and linear distributions of porosity are particular cases, and in this study, we also consider other values of p. Generally, power index represents the order of variations of volume fraction and eventually other properties. Moreover, for illustration, in Fig. 2, we present the effects of power index on volume fraction for $\rho_p/\rho_s = 0.3$.

2.2 Kinematic formulation

In this work, consider the displacement field in three different directions (Mantari 2015; Mantari and Guedes Soares 2014):

$$\begin{gathered}
u_1(x, y, z, t) = u(x, y, t) - z\left[w_{b,x} + \left(f'\left(\frac{h}{2}\right) + g\left(\frac{h}{2}\right)\right) w_{s,x}\right] + f(z)\, w_{s,x}, \\
u_2(x, y, z, t) = v(x, y, t) - z\left[w_{b,y} + \left(f'\left(\frac{h}{2}\right) + g\left(\frac{h}{2}\right)\right) w_{s,y}\right] + f(z)\, w_{s,y}, \\
u_3(x, y, z, t) = w_b(x, y, t) + g(z)\, w_s(x, y, t), \\
f(z) = \frac{h}{m} \tan h(\frac{mz}{h}) + z^3, \\
g(z) = n f(z), \\
n = 2/15, m = 0.4,
\end{gathered} \tag{7}$$

where u, v, w_b, and w_s stand for midplane displacements in the x, y, z directions, bending the component and shear components of transverse displacements, respectively. Also, $f(z)$ and $g(z)$ are obtained using stress-free edge conditions on the top of the plate, and for details, we refer to Mantari and Guedes Soares (2014) and Mantari (2015). It is worth mentioning that the number of unknowns is four, which is less than in FSDT and higher-order shear deformation theory (HSDT).

The linear strain-displacement components are expressed as (Mantari and Guedes Soares 2014; Mantari 2015)

$$\left\{\begin{array}{c}\varepsilon_x\\ \varepsilon_y\\ \gamma_{xy}\end{array}\right\}=\left\{\begin{array}{c}u_{,x}\\ v_{,y}\\ u_{,y}+v_{,x}\end{array}\right\}-z\left(\left\{\begin{array}{c}w_{b,xx}\\ w_{b,yy}\\ 2w_{b,xy}\end{array}\right\}+\left(f'(\frac{h}{2})+g(\frac{h}{2})\right)\left\{\begin{array}{c}w_{s,xx}\\ w_{s,yy}\\ 2w_{s,xy}\end{array}\right\}\right) \tag{8}$$

$$-f(z)\left\{\begin{array}{c}w_{s,xx}\\ w_{s,yy}\\ 2w_{s,xy}\end{array}\right\},$$

$$\varepsilon_z=g'(z)w_s,$$

$$\left\{\begin{array}{c}\gamma_{yz}\\ \gamma_{xz}\end{array}\right\}=\left\{\begin{array}{c}\left(-f'(\frac{h}{2})+g(\frac{h}{2})+g(z)+f'(z)\right)w_{s,y}\\ \left(-f'(\frac{h}{2})+g(\frac{h}{2})+g(z)+f'(z)\right)w_{s,x}\end{array}\right\},$$

where ε_i $(i=x,y,z)$ and γ_i $(i=xy,yz,xz)$ stand for the normal and shear strains, respectively. Clearly, the normal strain through the thickness direction is proportional to the shear component of transverse displacement, a polynomial and trigonometric hyperbolic function in the thickness direction.

3 Governing equations

In this section, we derive the governing equations of motions of FGV open-cell foam plates on visco-Pasternak foundation considering thickness-stretching effect. To this aim, we implement the dynamic version of virtual displacement or Hamilton principle:

$$\int_{t_1}^{t_2}(\delta U+\delta V-\delta T)dt=0,$$

$$\delta U=\int_A\int_{-h/2}^{h/2}\left(\begin{array}{l}\sigma_{xx}(\omega)\delta\varepsilon_x+\sigma_{yy}(\omega)\delta\varepsilon_y+\sigma_{zz}(\omega)\delta\varepsilon_z\\ +\sigma_{xy}(\omega)\delta\varepsilon_{xy}+\sigma_{yz}(\omega)\delta\varepsilon_{yz}+\sigma_{xz}(\omega)\delta\varepsilon_{xz}\end{array}\right)dzdA,$$

$$\delta V=\int_A\int_{-h/2}^{h/2}(K_w\delta u_3-K_p\left(u_{3,x}\delta u_{3,x}+u_{3,y}\delta u_{3,y}\right)+K_d u_{3,t}\delta u_{3,t})dzdA, \tag{9}$$

$$\delta T=\int_A\int_{-h/2}^{h/2}\rho(z,\omega)(u_{1,t}\delta u_{1,t}+u_{2,t}\delta u_{2,t}+u_{3,t}\delta u_{3,t})dzdA,$$

$$\delta u_i=0,(u_i=u,v,w_b,w_s),$$

where A, t_1, t_2, δu_i, δU, δV, and δT denote the area, initial time, terminal time, virtual displacement, virtual strain energy, potential energy of foundation, and virtual kinematic energy, respectively. Substituting Eqs. (1)–(8) into Eqs. (9), integrating in the thickness direction, and integrating by parts, we can extract the virtual displacements and write the resulting equations of motions as

$$
\begin{aligned}
\delta u &: N_{x,x}(\omega) + N_{xy,y}(\omega) \\
&= I_0(\omega)\, u_{,tt} - I_1(\omega)\, w_{b,xtt} \\
&\quad + \left(I_3(\omega) - \left(f'\left(\frac{h}{2}\right) + g\left(\frac{h}{2}\right)\right) I_1(\omega)\right) w_{s,xtt},
\end{aligned}
\tag{10}
$$

$$
\begin{aligned}
\delta v &: N_{xy,x}(\omega) + N_{y,y}(\omega) \\
&= I_0(\omega)\, v_{,tt} - I_1(\omega)\, w_{b,ytt} \\
&\quad + \left(I_3(\omega) - \left(f'\left(\frac{h}{2}\right) + g\left(\frac{h}{2}\right)\right) I_1(\omega)\right) w_{s,ytt},
\end{aligned}
\tag{11}
$$

$$
\begin{aligned}
\delta w_b &: M_{x,xx}(\omega) + 2M_{xy,xy}(\omega) + M_{y,yy}(\omega) \\
&= I_0(\omega) w_{b,tt} + I_1(\omega)\left(u_{,x} + v_{,y}\right)_{,tt} - I_2(\omega)\nabla^2 w_{b,tt} \\
&\quad + \left(I_4(\omega) - I_2(\omega)(f'(h/2) + g(h/2)\right)\nabla^2 w_{s,tt} + I_6(\omega) w_{s,tt} \\
&\quad + K_w\left(w_b + g(h/2) w_s\right) - K_p\left(\nabla^2 w_b + g\left(\frac{h}{2}\right)\nabla^2 w_s\right) \\
&\quad + K_d\left(w_{b,t} + g\left(\frac{h}{2}\right) w_{s,t}\right),
\end{aligned}
\tag{12}
$$

$$
\begin{aligned}
\delta w_s &: \left(f'(h/2) + g(h/2)\right)\left(M_{x,xx}(\omega) + 2M_{xy,xy}(\omega) + M_{y,yy}(\omega)\right. \\
&\quad \left. - N_{xz,x}(\omega) - N_{yz,y}(\omega)\right) - P_{x,xx}(\omega) - 2P_{xy,xy}(\omega) - P_{y,yy}(\omega) + Q_{yz,y}(\omega) \\
&\quad + Q_{xz,x}(\omega) + K_{yz,y}(\omega) + K_{xz,x}(\omega) - R_z(\omega) \\
&= -\left(I_3(\omega) - I_1(\omega)(f'(h/2) + g(h/2)\right)\left(u_{,x} + v_{,y}\right)_{,tt} \\
&\quad + \left(I_4(\omega) - I_2(\omega)(f'(h/2) + g(h/2)\right)\nabla^2 w_{b,tt} \\
&\quad + \left(-\left(f'(h/2) + g(h/2)\right)^2 I_2 + 2\left(f'(h/2) + g(h/2)\right) I_4 - I_5\right)\nabla^2 w_{s,tt} \\
&\quad + I_6 w_{b,tt} + I_7 w_{s,tt} \\
&\quad + g\left(\frac{h}{2}\right) K_w\left(w_b + g\left(\frac{h}{2}\right) w_s\right) - g\left(\frac{h}{2}\right) K_p\left(\nabla^2 w_b + g\left(\frac{h}{2}\right)\nabla^2 w_s\right) \\
&\quad + g\left(\frac{h}{2}\right) K_d\left(w_{b,t} + g\left(\frac{h}{2}\right) w_{s,t}\right),
\end{aligned}
\tag{13}
$$

where N, M, Q, K, R, and I_i $(i = 0, \ldots, 6)$ stand for the frequency-dependent stress resultants and frequency-dependent mass inertia, respectively, which are defined as

$$
\left\{ \begin{matrix} N_i(\omega), M_i(\omega), P_i(\omega) \\ Q_j(\omega), K_j(\omega) \\ R_z(\omega) \end{matrix} \right\} = \int_{-\frac{h}{2}}^{\frac{h}{2}} \left\{ \begin{matrix} \sigma_i\,(1, z, f) \\ \sigma_j(g, f'(z)) \\ \sigma_z g_{,z} \end{matrix} \right\} dz \qquad \left(\begin{matrix} i = x, y, xy, yz, xz \\ j = xz, yz \end{matrix} \right),
\tag{14}
$$

$$\left\{\begin{array}{c} I_i(\omega) \\ I_j(\omega) \\ I_k(\omega) \end{array}\right\} = \int_{-\frac{h}{2}}^{\frac{h}{2}} \left\{\begin{array}{c} \rho z^i \\ \rho(f, zf, f^2) \\ \rho(g, g^2) \end{array}\right\} dz \quad \begin{pmatrix} i = 0, 1, 2 \\ j = 3, 4, 5 \\ k = 6, 7 \end{pmatrix}.$$

For the case of stress resultants, the extended form is rewritten as

$$\left\{\begin{array}{c} N_x \\ N_y \\ N_{xy} \\ M_x \\ M_y \\ M_{xy} \\ P_x \\ P_y \\ P_{xy} \\ R_z \end{array}\right\} = \begin{bmatrix} A_{11} & A_{12} & 0 & B_{11} & B_{12} & 0 & C_{11} & C_{12} & 0 & F_{12} \\ A_{12} & A_{11} & 0 & B_{12} & B_{11} & 0 & C_{12} & C_{11} & 0 & F_{12} \\ 0 & 0 & A_{66} & 0 & 0 & B_{66} & 0 & 0 & C_{66} & 0 \\ B_{11} & B_{12} & 0 & G_{11} & G_{12} & 0 & H_{11} & H_{12} & 0 & K'_{12} \\ B_{12} & B_{11} & 0 & G_{12} & G_{11} & 0 & H_{12} & H_{11} & 0 & K'_{12} \\ 0 & 0 & B_{66} & 0 & 0 & G_{66} & 0 & 0 & H_{66} & 0 \\ C_{11} & C_{12} & 0 & H_{11} & H_{12} & 0 & L_{11} & L_{12} & 0 & O_{12} \\ C_{12} & C_{11} & 0 & H_{12} & H_{11} & 0 & L_{12} & L_{11} & 0 & O_{12} \\ 0 & 0 & C_{66} & 0 & 0 & H_{66} & 0 & 0 & L_{66} & 0 \\ F_{12} & F_{12} & 0 & K'_{12} & K'_{12} & 0 & O_{12} & O_{12} & 0 & U_{11} \end{bmatrix} \left\{\begin{array}{c} \varepsilon^0_{xx} \\ \varepsilon^0_{yy} \\ \varepsilon^0_{xy} \\ \varepsilon^1_{xx} \\ \varepsilon^1_{yy} \\ \varepsilon^1_{xy} \\ \varepsilon^2_{xx} \\ \varepsilon^2_{yy} \\ \varepsilon^2_{xy} \\ \varepsilon_{zz} \end{array}\right\}, \tag{15}$$

$$\left\{\begin{array}{c} N_{yz} \\ N_{xz} \\ K_{yz} \\ K_{xz} \\ Q_{yz} \\ Q_{xz} \end{array}\right\} = \begin{bmatrix} A_{66} & 0 & D_{66} & 0 & E_{66} & 0 \\ 0 & A_{66} & 0 & D_{66} & 0 & E_{66} \\ E_{66} & 0 & Q'_{66} & 0 & S_{66} & 0 \\ 0 & E_{66} & 0 & Q'_{66} & 0 & S_{66} \\ D_{66} & 0 & P'_{66} & 0 & Q'_{66} & 0 \\ 0 & D_{66} & 0 & P'_{66} & 0 & Q'_{66} \end{bmatrix} \left\{\begin{array}{c} \varepsilon^0_{yz} \\ \varepsilon^0_{xz} \\ \varepsilon^3_{yz} \\ \varepsilon^3_{xz} \\ \varepsilon^4_{yz} \\ \varepsilon^4_{xz} \end{array}\right\}, \tag{16}$$

where the matrix coefficients and strains are defined as

$$\begin{aligned} (A_i, B_i, C_i, D_i, E_i, F_i, G_i) &= \int_{-h/2}^{h/2} Q_{ij}(z)\left(1, z, f(z), g(z), f'(z), g'(z), z^2\right) dz, \\ \left(H_i, K'_i, L_i, O_i, U_i\right) &= \int_{-\frac{h}{2}}^{\frac{h}{2}} Q_{ij}(z)\left(zf(z), zg'(z), f^2(z), f(z)g'(z), g'^2(z)\right) dz, \\ \left(Q'_i, S_i, P'_i\right) &= \int_{-h/2}^{h/2} Q_{ij}(z)\left(g(z)f'(z), f'^2(z), g^2(z)\right) dz, \end{aligned} \tag{17}$$

$$\left\{\begin{array}{c} \varepsilon^0_{xx} \\ \varepsilon^0_{yy} \\ \varepsilon^0_{xy} \\ \varepsilon^1_{xx} \\ \varepsilon^1_{yy} \\ \varepsilon^1_{xy} \\ \varepsilon^2_{xx} \\ \varepsilon^2_{yy} \\ \varepsilon^2_{xy} \\ \varepsilon_z \end{array}\right\} = \left\{\begin{array}{c} u_{,x} \\ v_{,y} \\ u_{,y} + v_{,x} \\ -w_{b,xx} - \left(f'(h/2) + g(h/2)\right) w_{s,xx} \\ -w_{b,yy} - \left(f'(h/2) + g(h/2)\right) w_{s,yy} \\ -2w_{b,xy} - 2\left(f'(h/2) + g(h/2)\right) w_{s,xy} \\ w_{s,xx} \\ w_{s,yy} \\ 2w_{s,xy} \\ w_s \end{array}\right\}, \tag{18}$$

$$\begin{Bmatrix} \varepsilon_{yz}^0 \\ \varepsilon_{xz}^0 \\ \varepsilon_{yz}^3 \\ \varepsilon_{xz}^3 \\ \varepsilon_{yz}^4 \\ \varepsilon_{xz}^4 \end{Bmatrix} = \begin{Bmatrix} -\left(f'(h/2)+g(h/2)\right) w_{s,y} \\ -\left(f'(h/2)+g(h/2)\right) w_{s,x} \\ w_{s,y} \\ w_{s,x} \\ w_{s,y} \\ w_{s,x} \end{Bmatrix}. \tag{19}$$

Also, the displacement field variables are expressed based on harmonic functions as (Rao 2004)

$$\begin{aligned} u(x,y,t) &= u(x,y)e^{i\omega t}, \\ v(x,y,t) &= v(x,y)\,e^{i\omega t}, \\ w_b(x,y,t) &= w_b(x,y)\,e^{i\omega t}, \\ w_s(x,y,t) &= w_s(x,y)\,e^{i\omega t}. \end{aligned} \tag{20}$$

By substitution of strains (18)–(19) into the resultant equations (15)–(16), using harmonic functions, we can rewrite the governing equations (10)–(13) as

$$\begin{aligned} & A_{11}u_{,xx} + A_{66}u_{,yy} + (A_{12}+A_{66})\,v_{,xy} - B_{11}\nabla^2 w_{b,x} + (B_{11}q_{11}+C_{11})\,\nabla^2 w_{s,x} \\ & \quad + F_{12}w_{s,x} - \omega^2\left(-I_0u + I_1w_{b,x} + (I_3 - I_1q_{11})\,w_{s,x}\right) = 0, \end{aligned} \tag{21}$$

$$\begin{aligned} & (A_{12}+A_{66})\,u_{,xy} + A_{66}v_{,xx} + A_{11}v_{,yy} - B_{11}\nabla^2 w_{b,y} + (B_{11}q_{11}+C_{11})\,\nabla^2 w_{s,y} \\ & \quad + F_{12}w_{s,y} - \omega^2\left(-I_0v + I_1w_{b,y} + (I_3 - I_1q_{11})\,w_{s,y}\right) = 0, \end{aligned} \tag{22}$$

$$\begin{aligned} & B_{11}\nabla^2 u_{,x} + B_{11}\nabla^2 v_{,y} + G_{11}\left(q_{11}\nabla^4 w_s - \nabla^4 w_b\right) + H_{11}\nabla^4 w_s + K'_{12}\nabla^2 w_s \\ & \quad - (K_w + i\omega K_d)\,(w_b + g(h/2)w_s) + K_p\left(\nabla^2 w_b + g(h/2)\nabla^2 w_s\right) \\ & \quad - \omega^2\left(-I_0w_b - I_1u_{,x} - I_1v_{,y} + I_2\nabla^2 w_b + (I_4 - q_{11}I_2)\,\nabla^2 w_s - I_6w_s\right) = 0, \end{aligned} \tag{23}$$

$$\begin{aligned} & -C_{11}\nabla^2\left(u_{,x}+v_{,y}\right) - F_{12}\left(u_{,x}+v_{,y}\right) + q_{11}B_{11}\nabla^2\left(u_{,x}+v_{,y}\right) \\ & \quad + (H_{11} - G_{11}q_{11})\,\nabla^4 w_b + K'_{12}\nabla^2 w_b - g(h/2)\big((K_w + i\omega K_d)\,(w_b + g(h/2)w_s) \\ & \quad - K_p\left(\nabla^2 w_b + g(h/2)\nabla^2 w_s\right)\big) \\ & \quad + \left(-q_{11}^2A_{66} + 2Q'_{66} + P'_{66} - 2O'_{12} + S'_{66}\right)\nabla^2 w_s + \left(q_{11}^2G_{11} - L_{11}\right)\nabla^4 w_s - U_{11}w_s \\ & \quad - \omega^2\big((I_3 - I_1q_{11})\left(u_{,x}+v_{,y}\right) + (q_{11}I_2 - I_4)\,\nabla^2 w_b - I_6w_b \\ & \quad + I_5\nabla^2 w_s - I_7w_s + \left(q_{11}^2I_2 - 2q_{11}I_4\right)\nabla^2 w_s\big) = 0, \end{aligned} \tag{24}$$

$$\begin{aligned} & \nabla^2\,() = ()_{,xx} + ()_{,yy}\,, \\ & \nabla^4\,() = \nabla^2\left(\nabla^2\,()\right) = ()_{,xxxx} + 2\,()_{,xxyy} + ()_{,yyyy}\,, \end{aligned} \tag{25}$$

where $\nabla^2\,()$ and $\nabla^4\,()$ stand for the Nabla and biharmonic operators, respectively.

4 Semianalytical solution

In this section, we resolve the mentioned governing equations of motions using the Bubnov–Galerkin method and QZ eigenvalue solver (Golub and Van Loan 2013) to obtain fundamental frequencies and modal loss factors of foam plates with simply supported boundary conditions. The introduced edge conditions are defined as

$$\begin{aligned} N_x = M_x = P_x = v = w_b = w_s = w_{s,y} = 0, \quad x = 0, a, \\ N_y = M_y = P_y = u = w_b = w_s = w_{s,x} = 0, \quad y = 0, b. \end{aligned} \tag{26}$$

By applying the Galerkin weighed residual method, we discretize four-coupled PDEs of motion in the spatial domain. The applied functions of movable simply supported edge conditions are (Mantari 2015)

$$\begin{aligned} u(x,y) &= \cos(\frac{m\pi}{a}x)\sin(\frac{n\pi}{b}y), \\ v(x,y) &= \sin(\frac{m\pi}{a}x)\cos(\frac{n\pi}{b}y), \\ w_b(x,y) &= \sin(\frac{m\pi}{a}x)\sin(\frac{n\pi}{b}y), \\ w_s(x,y) &= \sin(\frac{m\pi}{a}x)\sin(\frac{n\pi}{b}y). \end{aligned} \tag{27}$$

The degraded PDEs of motions convert to a system of complex algebraic equations with frequency-dependent coefficients. The system of equations can be rewritten as

$$\big(\boldsymbol{C}(\omega) - \omega^2 \boldsymbol{M}(\omega) + \boldsymbol{C}'(\omega)\big)\,\boldsymbol{q} = 0, \tag{28}$$

where $\mathbf{C}$, $\boldsymbol{C}'$, $\mathbf{M}$, and $\mathbf{q}$ stand for the square matrices of frequency-dependent stiffness, damping, inertia, and vector of displacement, respectively. By applying QZ eigenvalue solver the outcomes are complex roots, which are written as (Zamani and Aghdam 2016)

$$\begin{aligned} \omega &= \omega^{\mathrm{Re}} + i\omega^{\mathrm{Im}}, \\ \omega_{mn} &= \omega^{\mathrm{Re}}, \\ \eta &= \frac{2\omega^{\mathrm{Re}}\omega^{\mathrm{Im}}}{(\omega^{\mathrm{Re}})^2 - (\omega^{\mathrm{Im}})^2}, \end{aligned} \tag{29}$$

where η and superscripts Re, Im stand for the modal loss factor and real and imaginary parts of frequencies, respectively. Furthermore, the real and imaginary parts of complex frequencies refer to the natural frequency and damping capability, respectively. In this study, damping emanates from two sources: first, material damping due to viscoelasticity, and the second is external damping of foundations.

5 Results and discussion

In this part, the presented method is verified and the impacts of various parameters are evaluated through numerical examples. First, the present method is verified for available results of elastic Al/Al_2O_3 plate on an elastic foundation (Thai and Choi 2012; Akavci 2014; Mantari et al. 2014b,a; Alazwari and Zenkour 2022) and laminated viscoelastic composite plate (Koo and Lee 1993). Then the impacts of geometry and foundation on complex frequencies are studied with numerical examples. We further assume the following properties of FGV open-cell foam plates: $\rho_p/\rho_s = 0.65$, $\rho_s = 200\ \text{kg/m}^3$, $G_0 = 2$ GPa, $K_0 = 2G_0$, $h = 1$, $\beta = 0.5$, $b/a = 1$, $a/h = 10$, $p = 1$, $(m, n) = (1, 1)$.

5.1 Comparative studies

In this section, we compare the nondimensional fundamental frequency parameters of elastic Al/Al_2O_3 plates with available results reported by Thai and Choi (2012), Akavci (2014), Mantari et al. (2014a), Mantari et al. (2014b), and Alazwari and Zenkour (2022). For this case, the assumed properties and parameters are as follows: $E_m = 70$ GPa, $\rho_m = 2702\ \text{kg/m}^3$, $E_c = 380$ GPa, $\rho_c = 3800\ \text{kg/m}^3$, $\nu = 0.3$, $\bar{K}_w = \frac{K_w a^4}{D_m}$, $\bar{K}_s = \frac{K_s a^4}{D_m}$, $D_m = \frac{E_m h^3}{12(1-\nu^2)}$, $\bar{\omega} = \frac{\omega a^2}{h}\sqrt{\rho_m/E_m}$. The obtained results are compared in Table 1. As we can see, by increment of side-to-thickness ratio and aspect ratio the frequencies increase. Also, by adding the elastic foundation frequencies enlarge, whereas by increment of power index frequencies decrease. Moreover, it is revealed that the aspect ratios have more impacts on frequencies than the side-to-thickness ratios.

The next example studies the nondimensional natural frequencies $\omega' = a^2/h(\rho/E_2)^{1/2}$ and modal loss factors of laminated viscoelastic composite plates with $[0]_{8T}$ layers, and material properties are (Koo and Lee 1993): $\rho = 1566\ \text{kg/m}^3$, $V_f = 0.516$, $h = 1.58$ mm, $a = b = 200$ mm, $\nu_{12} = 0.3$, $E_1 = 172.7(1 + 0.0007162i)$, $E_2 = 7.2(1 + 0.0067816i)$, $G_{12} = G_{23} = 3.76(1 + 0.01122i)$. The results are collated in Fig. 3, and a reliable correlation is observed between the present result and those obtained via Mindlin plate theory. It should be mentioned that the present study represents lower natural frequencies and higher loss factors than Mindlin theory due to greater flexibility of SNDT than Mindlin theory. Also, the presented results have no significant differences because the considered composite plates are very thin. After verification in elastic and viscoelastic domains, the effects of parameters on vibrational characteristics could be evaluated via a set of parametric study.

5.2 Parametric studies

In this part, we study the effects of parameters of aspect ratio (b/a), thickness ratio (a/h), power index, and foundation coefficients via numerical examples.

First, the fundamental frequencies and loss factors versus aspect ratio of FGV foam plates with different power indices are depicted in Fig. 4.

As we can see, both frequencies and loss factors decrease as the aspect ratio increases. Also, long rectangular narrow foam plates have lower values of stiffness and damping capability. However, the maximum and minimum reductions of frequencies are 49.07% and 40.46%, which refer to plates with $p = 1, 5$, respectively. In other words, plates with linear distribution of porosity are more sensitive to the aspect ratios. The counterpart values of loss factors are 48% and 38% for $p = 0, 5$, respectively. In other words, the loss factors of homogenous plates are the most affected by the aspect ratio. Moreover, foam plates with long aspect ratios have lower damping capability.

Second, the effects of thickness ratio on natural frequencies and loss factors are presented in Fig. 5. By increment of thickness ratio fundamental frequencies increase; in other words, frequencies of thin plates are larger than those of thick plates. However, thin plates have lower loss factor or damping capability than that of thick plates. Among considered

Table 1 A comparison of the frequency parameters $\bar{\omega}$ of Al/Al_2O_3 plates on elastic foundation

			$p=0$			$p=1$					
$\bar{K}_w, \bar{K}_p$	a/b	a/h	Ref[a]	Ref[b]	Present	Ref[a]	Ref[b]	Ref[c]	Ref[d]	Ref[e]	Present
0, 0	0.5	5	6.7610	6.7771	6.9836	5.2016	5.2122	5.2875	5.2018	5.28772	5.1830
		10	7.1746	7.1794	7.0314	5.4887	5.4918	5.5728	5.4887	5.57286	5.3537
		20	7.2936	7.2948	8.1472	5.5704	5.5712	5.6538	5.5704	5.65379	6.2253
	1	5	10.3761	10.4133	10.8207	8.0122	8.0368	8.1509	8.0127	8.15131	8.3102
		10	11.3351	11.3468	11.4775	8.6824	8.6899	8.8178	8.6825	8.81788	8.8546
		20	11.6307	11.6338	11.6550	8.8859	8.8879	9.0196	8.8859	9.01959	9.0071
	2	5	22.7045	22.8734	27.0728	17.7148	17.8289	18.0607	17.7181	18.0627	20.5980
		10	27.0439	27.1085	27.9347	20.8063	20.8487	21.1501	20.8071	21.15090	20.7321
		20	28.6985	28.7174	28.1257	21.9548	21.9670	22.2914	21.9550	22.29144	21.4151
0, 10^2	0.5	5	11.1150	11.1237	11.3349	10.8450	10.8489	10.7649	10.8451	10.76493	10.9442
		10	11.4474	11.4503	11.3584	11.0926	11.0940	11.1042	11.0926	11.10417	11.0351
		20	11.5467	11.5474	12.1065	11.1656	11.1660	11.1999	11.1656	11.19984	11.5070
	1	5	15.1867	15.2095	15.8031	14.3818	14.3923	14.2406	14.3820	14.24088	14.8660
		10	15.9732	15.9813	16.1998	14.9401	14.9443	14.9631	14.9402	14.96319	15.0556
		20	16.2263	16.2285	17.3901	15.1177	15.1189	15.1825	15.1177	15.18244	15.8550
	2	5	28.5409	28.6623	33.2002	25.6294	25.6912	25.2563	25.6312	25.25781	28.3028
		10	32.2917	32.3444	33.2264	28.2023	28.2316	28.2878	28.2028	28.28833	28.7568
		20	33.7917	33.8076	33.2709	29.2181	29.2272	29.4271	29.2182	29.42715	28.8632
10^2, 0	0.5	5	7.2126	7.2276	7.4363	5.8654	5.8746	5.9257	5.8655	5.92588	5.8638
		10	7.6108	7.6153	7.4727	6.1366	6.1393	6.2077	6.1366	6.20770	6.0217
		20	7.7260	7.7272	8.5368	6.2144	6.2152	6.2883	6.2145	6.28824	6.8078
	1	5	10.6723	10.7082	11.1306	8.4517	8.4748	8.5671	8.4522	8.56752	8.7704
		10	11.6147	11.6261	11.3258	9.1035	9.1107	9.2282	9.1036	9.22829	9.2689
		20	11.9062	11.99093	11.9268	9.3025	9.3044	9.4292	9.3025	9.42918	10.3375
	2	5	22.8378	23.0053	27.2205	17.9108	18.0231	18.2385	17.9141	18.24050	20.8162
		10	27.1603	27.2246	28.0514	20.9821	21.0241	21.3187	20.9829	21.31945	21.5919
		20	28.8106	28.8295	28.2393	22.1257	22.1378	22.4585	22.1258	22.45857	21.6414
10^2, 10^2	0.5	5	11.3952	11.4036	11.6144	11.1780	11.1817	11.0894	11.1781	11.08946	11.2836
		10	11.7257	11.7285	11.6400	11.4270	11.4284	11.4358	11.4270	11.43582	11.3696
		20	11.8246	11.8253	12.3720	11.5005	11.5008	11.5331	11.5005	11.53311	11.8322
	1	5	15.3904	15.4127	15.9569	14.6305	14.6407	14.4792	14.6307	14.47947	15.1176
		10	16.1728	16.1808	16.0117	15.1887	15.1927	15.2084	15.1887	15.20848	15.3031
		20	16.4249	16.4271	16.3966	15.3663	15.3674	15.4293	15.3663	15.42927	16.0924
	2	5	28.6467	28.7674	33.2982	25.7640	25.8251	25.3782	25.7657	25.37974	28.4354
		10	32.3893	32.4417	33.3332	28.3322	28.3613	28.4137	28.3327	28.41429	28.8874
		20	33.8869	33.9029	33.3670	29.3467	29.3557	29.5539	29.3469	29.55394	28.9941

[a] Thai and Choi (2012); [b] Akavci (2014); [c] Mantari et al. (2014a); [d] Mantari et al. (2014b); [e] Alazwari and Zenkour (2022).

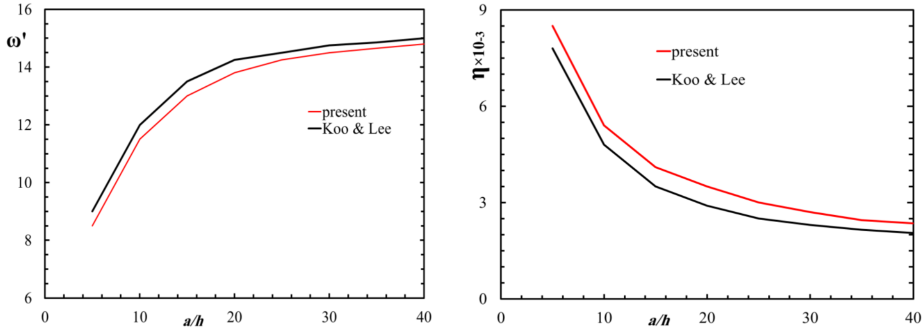

Fig. 3 A comparison of fundamental frequencies and loss factors of laminated composite plates versus side-to-thickness ratio

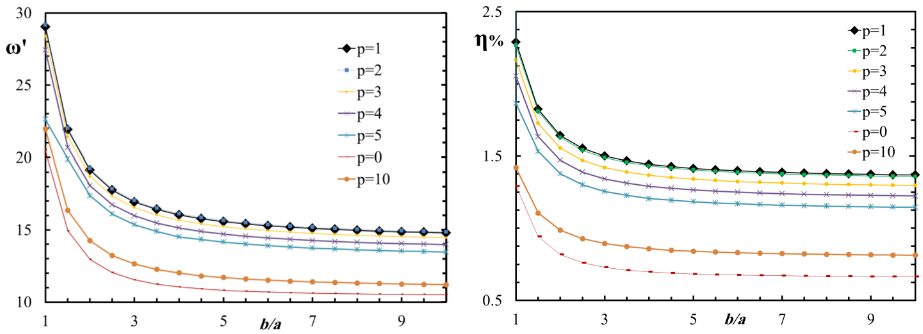

Fig. 4 Vibrational characteristics of plates with different aspect ratios and power indices

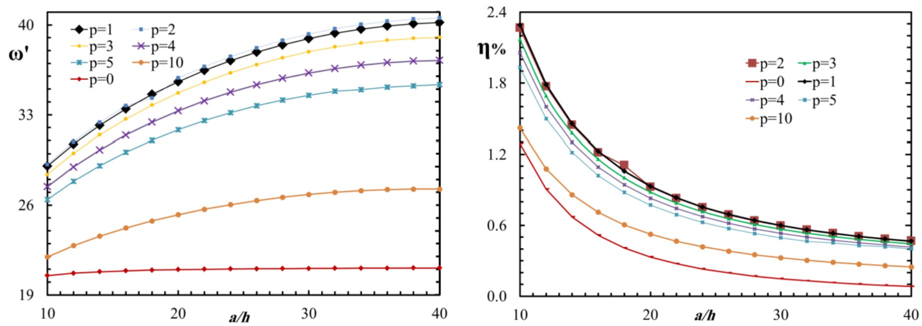

Fig. 5 Vibrational characteristics of plates with different side-to-thickness ratios and power indices

plates, the plates with linear and parabolic distributions of porosities have the maximum fundamental vibrational characteristics. On the contrary, foam plates with drastic variations of properties or higher values of power index have lower natural frequencies and damping capability.

Third, the impacts of power index and material models are investigated by Fig. 6. As depicted, both models have the maximum frequencies at $p = 2$, whereas the material model

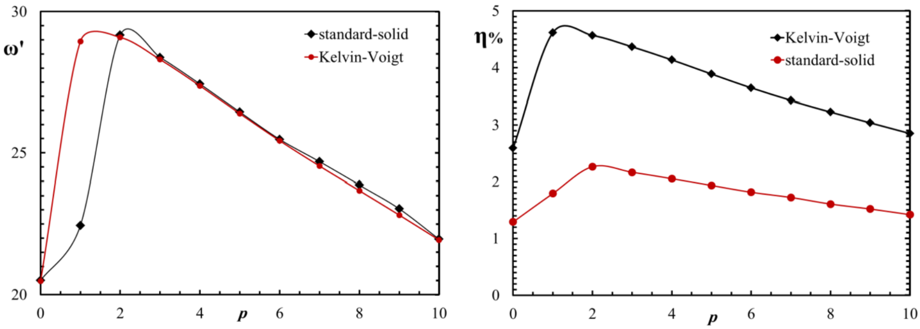

Fig. 6 Vibrational characteristics of plates with different power index and model

has no significant effects on natural frequencies. On the contrary, the material model has remarkable effects on loss factors. Indeed, the Kelvin–Voigt model predicts higher loss factor than the standard solid model. Also, the maximum loss factor of Kelvin–Voigt refers to $p = 1$, and the maximum loss factor of standard solid refers to $p = 2$. In other words, the material model is the key factor for damping analysis, regardless the functions of porosity distribution.

Fourth, the effects of foundation are considered in Fig. 7 for plates in three cases. For the first case, $K_w = 0, 10^2, 10^3, 5000$, $K_p = K_d = 0$, for the second case, $K_w = 10^3$, $K_p = 0, 50, 10^2, 250$, $K_d = 0$, for the last case, $K_w = 10^3$, $K_p = 10^2$, $K_d = 0, 10^{-3}, 5 \times 10^{-3}, 10^{-2}$ are assumed. As we can observe, the fundamental frequencies increase as the thickness ratio increases. However, based on the assumed values of foundation stiffness, the Pasternak coefficients lead to remarkable distinction of frequencies, whereas the Winkler coefficients have lower impacts.

In addition, these values of damping coefficients result in no remarkable change of frequencies. For the loss factor, some interesting remarks are observed. Although it is mentioned that thin plates without foundation have lower damping capability, this remark is reliable to some extent for plates on viscoelastic foundation. Indeed, this behavior is true for elastic foundations, whereas, as both thickness ratio and viscoelastic coefficients promote, thin plates show an incremental approach of loss factors. The main reason refers to the fact that external damping outweighs material damping. So the loss factors reach their minimum points and then follow an incremental approach. It is worth mentioning that the minimum points refer to $a/h = 10, 12, 20$, and 40 for $K_d = 10^{-2}, 5 \times 10^{-3}, 10^{-3}$, and 0, respectively.

Fifth, the behaviors of higher-mode of vibrations are studied in Fig. 8. For this case, $K_w = 10^3$, $K_p = 10^2$, and $K_d = 10^{-3}$ are assumed. For this example, the minimum value of loss factors of $(1,1)$. $(1,2)$, $(2,2)$, $(1,3)$, and $(2,3)$ modes refer to $a/h = 18, 28, 40, 44$, and 50, respectively. From damping capability point of view, fundamental modes are the most important modes due to remarkable variations of loss factors. In addition, it is clear that higher modes of plates on viscoelastic foundation are less sensitive to the thickness ratio variation. Besides, fundamental modes display thoroughly obvious behavior in comparison with higher mode of vibrations. Moreover, the curves of loss factors pass each other, which is known as the crossing phenomenon (Leissa 1974; Perkins and Mote 1986). Therefore here the crossing phenomenon of FGV foam plates on viscoelastic foundation is reported for the first time.

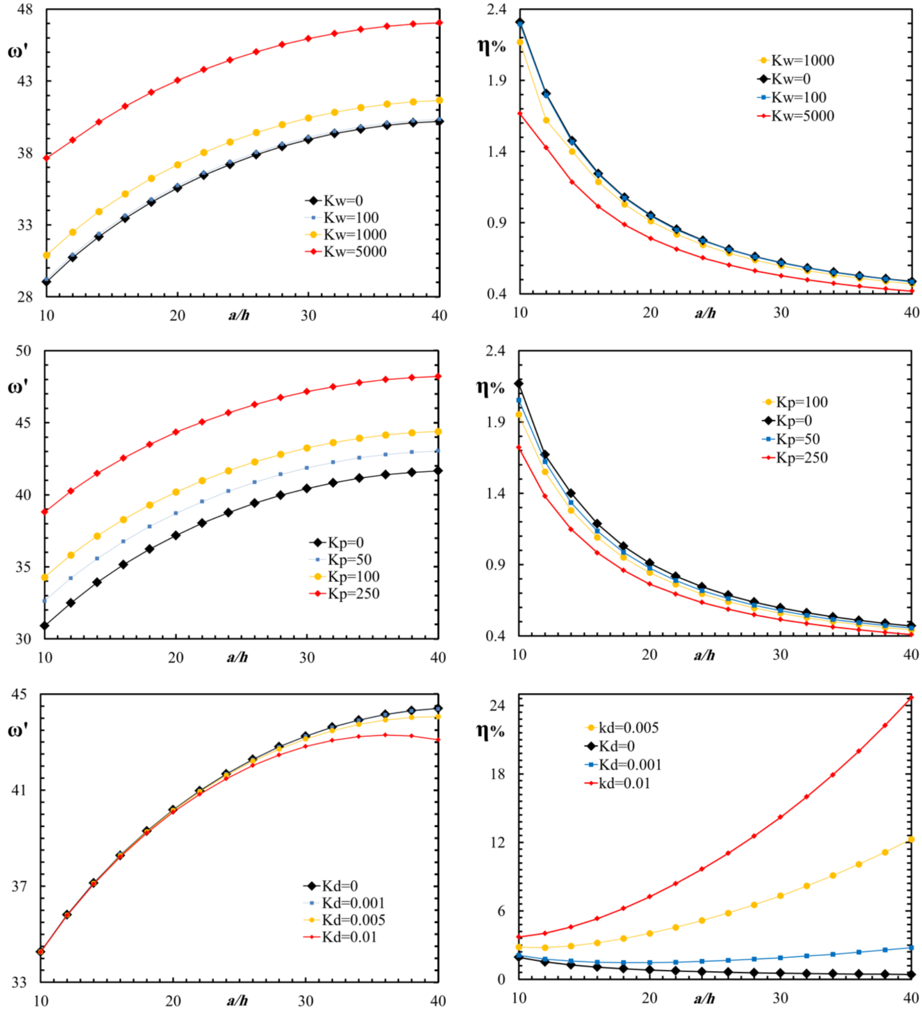

Fig. 7 Vibrational characteristics versus side-to-thickness ratio of plates on the viscoelastic foundation

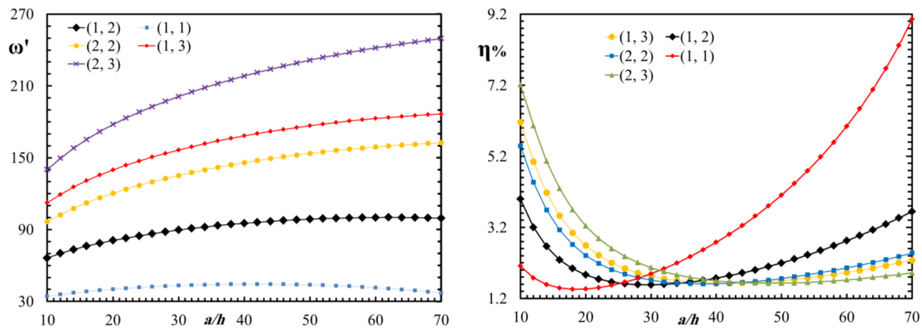

Fig. 8 The higher modes of plates on the viscoelastic foundations

6 Conclusions

The free vibration behavior of FGV open-cell foam plate on viscoelastic foundations is studied based on thickness-stretching effect. Boltzmann superposition principle, separable kernel framework, and simple power law are used to derive constitutive relations, and the Hamilton principle is implemented to obtain integro-PDEs of motion. The Galerkin method and the iterative numerical algorithm are applied to derive complex frequencies. For comparison, elastic FG plates on Pasternak foundation and laminated viscoelastic composite plates are studied. Based on new results, some conclusions are derived:

- Long rectangular narrow foam plates have smaller frequencies and loss factors than wide plates.
- Aspect ratios are the most effective on plates with linear distribution of porosity and on loss factors of homogenous plates.
- FGV plates with linear and parabolic distributions of porosities have the maximum fundamental frequencies and loss factors.
- Regardless of the porosity distribution, the material model is the key factor for damping analysis.
- Based on the values, Pasternak, Winkler, and damping coefficients are the most remarkable factor on frequencies.
- Loss factors of thin plates display an incremental approach as both thickness ratio and viscoelastic coefficients increase due to outweighing external damping over structural damping.
- The crossing phenomenon of FGV foam plates on viscoelastic foundation is observed.

Author contributions H. A. Zamani: Conceptualization, Methodology, Software, Writing - Original Draft, Writing - Review & Editing, M. Salehi: Conceptualization, Writing - Review & Editing.

Funding This research did not receive any specific grant from funding agencies in the public, commercial, or not-for-profit sectors.

Declarations

Competing interests The authors declare no competing interests.

References

Akavci, S.S.: An efficient shear deformation theory for free vibration of functionally graded thick rectangular plates on elastic foundation. Compos. Struct. **108**, 667–676 (2014). https://doi.org/10.1016/j.compstruct.2013.10.019

Alavi, S.K., Ayatollahi, M.R., Petrů, M., Koloor, S.S.R.: On the dynamic response of viscoelastic functionally graded porous plates under various hybrid loadings. Ocean Eng. **264**, 112541 (2022). https://doi.org/10.1016/j.oceaneng.2022.112541

Alazwari, M.A., Zenkour, A.M.: A quasi-3D refined theory for the vibration of functionally graded plates resting on visco-Winkler–Pasternak foundations. Mathematics **10**(5), 716 (2022)

Alfrey, T.: Non-homogeneous stresses in viscoelastic media. Q. Appl. Math. **2**(2), 113–119 (1944). https://doi.org/10.1090/qam/10499

Alimirzaei, S., Sadighi, M., Nikbakht, A.: Wave propagation analysis in viscoelastic thick composite plates resting on visco-Pasternak foundation by means of quasi-3D sinusoidal shear deformation theory. Eur. J. Mech. A, Solids **74**, 1–15 (2019). https://doi.org/10.1016/j.euromechsol.2018.10.012

Altenbach, H., Eremeyev, V.A.: Analysis of the viscoelastic behavior of plates made of functionally graded materials. J. Appl. Math. Mech. **88**(5), 332–341 (2008a). https://doi.org/10.1002/zamm.200800001

Altenbach, H., Eremeyev, V.A.: Direct approach-based analysis of plates composed of functionally graded materials. Arch. Appl. Mech. **78**(10), 775–794 (2008b). https://doi.org/10.1007/s00419-007-0192-3

Altenbach, H., Eremeyev, V.A.: On the bending of viscoelastic plates made of polymer foams. Acta Mech. **204**(3), 137 (2008c). https://doi.org/10.1007/s00707-008-0053-3

Altenbach, H., Eremeyev, V.A.: On the time-dependent behavior of FGM plates. Key Eng. Mater. **399**, 63–70 (2009). https://doi.org/10.4028/www.scientific.net/KEM.399.63

Ashby, M.F., Evans, A.G., Fleck, N.A., Gibson, L.J., Hutchinson, J.W., Wadley, H.N.G.: Metal Foams: A Design Guide, 1st edn. Butterworth-Heinemann, Woburn (2000)

Brinson, H.F., Brinson, L.C.: Polymer Engineering Science and Viscoelasticity an Introduction, 1st edn. Springer, Boston (2008)

Buratto, L., Giardini, P., Bellucci, R.: Viscoelastics in ophthalmic surgery. SLACK (2000)

Dogan, A.: Quasi-static and dynamic response of functionally graded viscoelastic plates. Compos. Struct. **280**, 114883 (2022). https://doi.org/10.1016/j.compstruct.2021.114883

Golub, G.H., Van Loan, C.F.: Matrix Computations, 4th edn. Johns Hopkins University Press, Baltimore (2013)

Hatami, S., Ronagh, H.R., Azhari, M.: Exact free vibration analysis of axially moving viscoelastic plates. Comput. Struct. **86**(17–18), 1738–1746 (2008). https://doi.org/10.1016/j.compstruc.2008.02.002

Hedayati, R., Sadighi, M.: A micromechanical approach to numerical modeling of yielding of open-cell porous structures under compressive loads. J. Theor. Appl. Mech. **54**(3), 769–781 (2016). https://doi.org/10.15632/jtam-pl.54.3.769

Hosseini-Hashemi, S., Abaei, A.R., Ilkhani, M.R.: Free vibrations of functionally graded viscoelastic cylindrical panel under various boundary conditions. Compos. Struct. **126**, 1–15 (2015). https://doi.org/10.1016/j.compstruct.2015.02.031

Jahwari, F.A., Naguib, H.E.: Analysis and homogenization of functionally graded viscoelastic porous structures with a higher order plate theory and statistical based model of cellular distribution. Appl. Math. Model. **40**(3), 2190–2205 (2016). https://doi.org/10.1016/j.apm.2015.09.038

Kerr, A.D.: Elastic and viscoelastic foundation models. J. Appl. Mech. **31**(3), 491–498 (1964). https://doi.org/10.1115/1.3629667

Koo, K.N., Lee, I.: Vibration and damping analysis of composite laminates using shear deformable finite element. AIAA J. **31**(4), 728–735 (1993). https://doi.org/10.2514/3.11610

Leissa, A.W.: On a curve veering aberration. J. Appl. Math. Phys. (ZAMP) **25**(1), 99–111 (1974). https://doi.org/10.1007/bf01602113

Mantari, J.L.: A refined theory with stretching effect for the dynamics analysis of advanced composites on elastic foundation. Mech. Mater. **86**, 31–43 (2015). https://doi.org/10.1016/j.mechmat.2015.02.010

Mantari, J.L., Guedes Soares, C.: Four-unknown quasi-3D shear deformation theory for advanced composite plates. Compos. Struct. **109**, 231–239 (2014). https://doi.org/10.1016/j.compstruct.2013.10.047

Mantari, J.L., Granados, E.V., Guedes Soares, C.: Vibrational analysis of advanced composite plates resting on elastic foundation. Composites, Part B, Eng. **66**, 407–419 (2014a). https://doi.org/10.1016/j.compositesb.2014.05.026

Mantari, J.L., Granados, E.V., Hinostroza, M.A., Guedes Soares, C.: Modelling advanced composite plates resting on elastic foundation by using a quasi-3D hybrid type HSDT. Compos. Struct. **118**, 455–471 (2014b). https://doi.org/10.1016/j.compstruct.2014.07.039

Montgomery, S.M., Hilborn, H., Hamel, C.M., Kuang, X., Long, K.N., Qi, H.J.: The 3D printing and modeling of functionally graded Kelvin foams for controlling crushing performance. Extreme Mech. Lett. **46**, 101323 (2021). https://doi.org/10.1016/j.eml.2021.101323

Perkins, N.C., Mote, C.D.: Comments on curve veering in eigenvalue problems. J. Sound Vib. **106**(3), 451–463 (1986). https://doi.org/10.1016/0022-460X(86)90191-4

Rao, S.S.: Mechanical Vibrations, 5th edn. Pearson Education, Upper Saddle River (2004)

Sadeghnejad, S., Taraz Jamshidi, Y., Mirzaeifar, R., Sadighi, M.: Modeling, characterization and parametric identification of low velocity impact behavior of time-dependent hyper-viscoelastic sandwich panels. Proc. Inst. Mech. Eng., L-J Mater. Des. Appl. **233**(4), 622–636 (2017). https://doi.org/10.1177/1464420716688233

Sarrafan, S., Li, G.: A hybrid syntactic foam-based open-cell foam with reversible actuation. ACS Appl. Mater. Interfaces (2022). https://doi.org/10.1021/acsami.2c16168

Shariyat, M., Jahangiri, M.: Nonlinear impact and damping investigations of viscoporoelastic functionally graded plates with in-plane diffusion and partial supports. Compos. Struct. **245**, 112345 (2020). https://doi.org/10.1016/j.compstruct.2020.112345

Singh, A., Naskar, S., Kumari, P., Mukhopadhyay, T.: Viscoelastic free vibration analysis of in-plane functionally graded orthotropic plates integrated with piezoelectric sensors: time-dependent 3D analytical solutions. Mech. Syst. Signal Process. **184**, 109636 (2023). https://doi.org/10.1016/j.ymssp.2022.109636

Sofiyev, A.: On the solution of dynamic stability problem of functionaly graded viscoelastic plates with different initial conditions in viscoelastic media. Mathematics (2023). https://doi.org/10.3390/math11040823
Sofiyev, A.H., Zerin, Z., Kuruoglu, N.: Dynamic behavior of FGM viscoelastic plates resting on elastic foundations. Acta Mech. (2019). https://doi.org/10.1007/s00707-019-02502-y
Srinivas, S., Rao, A.K.: An exact analysis of free vibrations of simply-supported viscoelastic plates. J. Sound Vib. **19**(3), 251–259 (1971). https://doi.org/10.1016/0022-460X(71)90687-0
Taraz Jamshidi, Y., Sadeghnejad, S., Sadighi, M.: Viscoelastic behavior determination of EVA elastomeric foams using FEA. In: 23rd Annu Int Conf Mech Eng-ISME. Amirkabir University of Technology, Tehran (2015)
Thai, H.-T., Choi, D.-H.: A refined shear deformation theory for free vibration of functionally graded plates on elastic foundation. Composites, Part B, Eng. **43**(5), 2335–2347 (2012). https://doi.org/10.1016/j.compositesb.2011.11.062
Zamani, H.A.: Free vibration of doubly-curved generally laminated composite panels with viscoelastic matrix. Compos. Struct. **258**, 113311 (2021a). https://doi.org/10.1016/j.compstruct.2020.113311
Zamani, H.A.: Free vibration of viscoelastic foam plates based on single-term Bubnov–Galerkin, least squares, and point collocation methods. Mech. Time-Depend. Mater. **25**(3), 495–512 (2021b). https://doi.org/10.1007/s11043-020-09456-y
Zamani, H.A.: Free vibration of functionally graded viscoelastic foam plates using shear- and normal-deformation theories. Mech. Time-Depend. Mater. (2022). https://doi.org/10.1007/s11043-021-09533-w
Zamani, H.A., Aghdam, M.M.: Hybrid material and foundation damping of Timoshenko beams. J. Vib. Control **23**(18), 2869–2887 (2016). https://doi.org/10.1177/1077546315624077
Zamani, H.A., Aghdam, M.M., Sadighi, M.: Free vibration of thin functionally graded viscoelastic open-cell foam plates on orthotropic visco-Pasternak medium. Compos. Struct. **193**, 42–52 (2018). https://doi.org/10.1016/j.compstruct.2018.03.061
Zamani, H.A., Nourazar, S.S., Aghdam, M.M.: Large-amplitude vibration and buckling analysis of foam beams on nonlinear elastic foundations. Mech. Time-Depend. Mater. (2022). https://doi.org/10.1007/s11043-022-09568-7